Superabundant vacancies in a metal-hydrogen system: Monte Carlo simulations

D. Tanguy[1,2,*] and M. Mareschal[2]
[1]*CNRS, UMR 5146, Ecole des Mines de Saint-Etienne, 158 cours Fauriel, Fr-42023 Saint-Etienne, France*
[2]*Centre Européen de Calcul Atomique et Moléculaire, Ecole Normale Supérieure, 46, Allée d'Italie, Fr-69007 Lyon, France*
(Received 11 April 2005; revised manuscript received 8 August 2005; published 30 November 2005)

An equilibrium Monte Carlo simulation capable of treating superabundant vacancy formation and ordering in metal-hydrogen systems (M-H) is developed. It combines lattice site occupations and continuous degrees of freedom which enables one to perform insertion/removal moves and hydrogen-vacancy cluster moves while the position of the particles are sampled. The bulk phase diagram in (μ_M, N_H, V, T) ensemble is estimated for concentrations lower than 1 at. %. Within the framework of an EAM Al-H potential, ordering of superabundant vacancies in the shape of chains and platelets is reported at room temperature.

DOI: 10.1103/PhysRevB.72.174116 PACS number(s): 61.72.Bb, 02.70.Uu, 61.72.Ji

I. INTRODUCTION

During the study of phase stability in metal hydrides, Fukai observed a deviation of the lattice parameter from the value of the hydride when the sample is held at high temperatures and high hydrogen pressures for a sufficiently long time. Lattice contractions have been measured in Pd-H (Ref. 1) and Ni-H (Ref. 2) and later in many other systems (see Ref. 3 for a review). The contraction was attributed to the diffusion of vacancies from the surface into the hydride. The vacancies are saturated with hydrogen, forming VH_6 vacancy hydrogen clusters containing six hydrogens in octahedral positions in Ni and Pd. Under the pressure conditions used, in the range of 1 to 5 GPa, the average hydrogen concentrations are higher than 50 at. % in most experiments. Therefore, hydrogen detrapping during vacancy-metal exchanges is probably not a strong obstacle to diffusion, enabling the system to reach the equilibrium vacancy concentration. The role of temperature is mainly to enable the system to overcome the barrier for vacancy production at the surface. After cooling at room temperature and hydrogen degassing, the large excess vacancy concentration (of the order of 10 at. %) precipitates in the form of bubbles. The authors[4] show from the size distribution and the concentration profile of the bubbles that they are undoubtedly related to vacancy diffusion from the surface and their subsequent precipitation after H desorption and not related to the formation of H_2 bubbles in the crystal. As these vacancy concentrations are orders of magnitude higher than the equilibrium concentrations without hydrogen, they are called superabundant vacancies (SAVs).

The high temperature is necessary to increase the vacancy formation kinetics but not to stabilize them. Indeed, in electrodeposited Ni, thermal desorption spectra (TDS) show hydrogen desorption peaks very similar to those obtained in Ni charged with hydrogen and vacancies at high temperature and pressure.[5] It seems that the electrodeposition process creates point defects at the surface, which are stabilized by adsorbed hydrogen and remain trapped in the metal as the sample is further grown by metal deposition. These superabundant vacancies are stable at room temperature. Even after several years, 1500 ppm of hydrogen has been released during TDS in Ni.[5] In Al, bulk hydrogen concentrations up to 500 ppm can be introduced by electrochemical charging without expansion of the lattice parameter.[6] This anomalous behavior and the small effective diffusion coefficient have been attributed to the formation of vacancy-hydrogen complexes that diffuse from the surface. Plasma charging showed that such complexes can diffuse from the implantation zone (limited to a 1 μm depth from the surface) inside the sample.[7] More generally, if the kinetics for vacancy production was faster, vacancy-hydrogen clusters would be observed in solids in contact with a high hydrogen fugacity instead of hydrogen in interstitial position.[3]

So far, the experimental studies focus on SAV formation in undeformed materials where internal vacancy sources are probably not activated. In hydrogen related crack propagation that involves a fast repassivation of the metal in aqueous media, it is well known that high hydrogen fugacities are produced locally. The fracture occurs in regions of high density of crystalline defects such as grain boundaries, precipitate-matrix interfaces, or localized slip bands where trapping is efficient and local hydrogen concentrations can be large. The microscopic reason for fracture is not fully understood. The effect of the vacancies created in the plastic zone ahead of the crack tip has been considered several times. Their production by a plastic process in fatigue has been recently confirmed by scanning positron microscope.[8,9] Nevertheless, the effect of vacancy-hydrogen clusters on the mechanical properties of metals have not been studied yet.

In this work, we develop a Monte Carlo method capable of producing the equilibrium concentration of superabundant vacancies (vacancy creation) as a function of the temperature and the bulk hydrogen concentration. In this method, the particles are not constrained to occupy the sites of a rigid lattice, but can be displaced to accommodate the stress fields of the vacancies and, eventually, of preexisting crystalline defects. The method is tested in bulk aluminum, using the embedded atom method (EAM). Al-H is a good test system because the vacancy formation energy is low and is easily compensated by the segregation of hydrogen. Therefore, large vacancy concentrations can be obtained at hydrogen concentrations corresponding to electrochemical charging. Furthermore, we investigate the ordering of the SAV. The possibility of the formation of clusters in {111} planes has been announced experimentally.[6,10] The method can be used

to investigate SAV equilibrium at dislocations and grain boundaries, in connection with the mechanical properties, but this is left for future work. As this kind of configuration requires a large number of particles, we use semiempirical interatomic potentials whose validity will be discussed. The method is exposed in two steps. First, we detail the statistical ensemble in which we develop a Monte Carlo algorithm for vacancy equilibration. The consistency of the method is tested by computing the vacancy concentration in pure Al at high temperature. The results are compared with those of an independent method. Second, interstitial solutes are included. An EAM Al-H potential is used as a generic model. The method is extended in order to handle vacancy-hydrogen clusters. Finally, the SAV equilibrium concentration, and order parameters, are computed as a function of the hydrogen concentration and temperature.

II. STATISTICAL MECHANICS

If we want to design an atomistic simulation which describes the statistics of SAV, the method has to handle the creation and deletion of a large number of vacancies, their ordering, and the local stress field they generate, in a way that is coherent with statistical mechanics.

The thermodynamics, statistical mechanics, and computer simulation of vacancies in crystals are detailed in Ref. 11. In this section, we briefly review the work of Swope and Andersen on the simulation of systems constrained by their number of lattice sites and the methodology they developed to treat vacancies efficiently in computer simulations. Then we present an Ising model with continuous degrees of freedom, which we will extend to treat the SAV problem. Finally, we compute vacancy concentrations with this model by Monte Carlo simulations. The concentrations found are in good agreement with the formation free energy of the vacancy computed by a particle insertion method.[12]

A. Constrained lattice, off-lattice method

Consider a macroscopic crystal where (N,V,T) are fixed. The system can equilibrate and get the adequate concentration of vacancies by the migration of atoms to the surface or by the activation of vacancy sources like grain boundaries or dislocations. By this mechanism, the number of lattice sites can increase in the crystal, at constant N, by an amount which corresponds to the formation of equilibrium vacancies in the bulk.

In small systems, (N,V,T) or (N,V,E) simulations of stable crystalline structures cannot produce the true number of vacancies because of the constraint related to the initial shape of the box, and the periodic boundary conditions. If the structure of the crystal is stable, creating net vacancies requires the formation of additional lattice sites generate improbable distortions of the lattice cell. Even if the creation of extra lattice sites was possible, the vacancy concentration could require a number of new lattice sites which does not correspond to an entire number of lattice planes. Therefore it would be incompatible with the periodic boundary conditions.

In the grand-canonical ensemble (μ,V,T), if the crystal structure is stable, the number of lattice sites is constant. The constraint will have an effect on the pressure-chemical potential relation. Let us imagine two sets of calculations at (μ,V,T) and $(\mu,V+\delta V,T)$. The virial pressure measured in these two series of simulations as a function of μ will be different, because the number of particles plus the number of vacancies is constrained to be equal to the number of lattice sites, which does not change for a small increase of the volume.

The thermodynamics of a crystal submitted to these constraints is developed in Ref. 11. An additional extensive variable is considered: M, the number of lattice sites. The thermodynamic state of the constraint system is specified by (N,V,T,M). A new intensive variable ν_c (c is the subscript for "constrained") is obtained by deriving the constrained Helmholtz free energy with respect to M. The correspondence with the thermodynamic properties of the unconstrained system is obtained formally when $\nu_c=0$ by adjusting the number of sites to minimize the free energy. This minimization gives $M_{eq}(N,V,T)$. Furthermore, the partition function of the constrained ensemble is given. Naturally, it is the same as the partition function in the (N,V,T) ensemble, but with the integration reduced to a subset of the phase space: the states that satisfy the constraint "structure and number of lattice sites imposed." It can be written[11]

$$\mathcal{Q}_c(N,V,T,M) = \frac{1}{N!h^{3N}} \int_V d\vec{r}^N \int d\vec{p}^N \delta\{M, m_N(\vec{r}^N,V)\} \times \exp[-\beta H_N(\vec{r}^N,\vec{p}^N)] \quad (1)$$

with

$$\mathcal{Q}(N,V,T) = \sum_M \mathcal{Q}_c(N,V,T,M), \quad (2)$$

where $m_N(\vec{r}^N,V)$ is the number of sites of the configuration defined by $(\vec{r}^N,V)$. Imagine that a long simulation is run in (N,V,T) on a large system. Each configuration can be analyzed to determine its crystalline structure. A lattice is defined and the particles are distributed over the lattice nodes. The empty lattice nodes are vacancies. Only the configurations that correspond to the specified structure and number of lattice nodes are to taken into account in Eq. (1).

To compute the unconstrained vacancy concentration, in practice, a set of simulations are performed according to the constrained probability distribution for a range of densities (number of particles per lattice sites) and volumes (per lattice site). The constrained virial pressure and chemical potential are computed, as well as one absolute free energy (by thermodynamic integration for example). With all these data, the chemical potential of the vacancies (ν_c) can be evaluated and the simulations that give the true vacancy concentration are detected by $\nu_c=0$.

The ability of producing the unconstrained vacancy concentration has proved to be crucial in the study of the stability of 2D crystals upon melting.[13] Because of long correlation times, close to the melting transition, it was found that the insertions and deletions of particles, performed in the

bicanonical ensemble,[11,14] efficiently speed up the equilibration of the structure. In classical grand canonical Monte Carlo (GCMC), the position for the insertion of a particle is selected at random. In dense systems where the repulsive interactions at short range are high, the probability that the insertion is accepted is low and the method is inefficient. The idea, originally proposed by Mezei,[15] is to detect the cavities in the system and perform biased insertions in them. In the bicanonical ensemble, a grid is generated separating physical space in small cells where the insertion are performed at random. In order to obtain high acceptance rates, a bias is introduced in the way of choosing which of the cells are adequate for insertion/deletion moves.[14] The boxes are then said to be ID cells (insertion/deletion).

From this review, we can keep in mind that, in a simulation, the system is constrained by its initial crystalline structure and the number of lattice sites in the simulation box. Therefore, only a subset of phase space is sampled. This is not a major drawback if the stability of the structure is preserved apart from local distortions, like those from vacancy clusters. Following this idea, we build a model where we impose a lattice, but allow the particles to have small displacements from the lattice nodes. This lattice has two roles: the empty nodes are the "cavities" where the particle insertions can be done more efficiently; it is a reference frame for local structure changes. The method is now detailed.

B. A lattice model with continuous degrees of freedom

In a macroscopic crystal, a vacancy is formed by taking a bulk atom and placing it in such a way that the chemical potential is not modified, for example, at a kink on a surface step. At constant pressure, the volume is relaxed and a contraction of the lattice is observed. The creation of the defect is done at constant (N,N_{H},p,T), where N is the total number of metal particles and N_{H}, the number of hydrogen particles. In the simulation it would be a prohibitive computational effort to mimic such a process. A way of simulating this situation is to consider the system in equilibrium with a reservoir that imposes the temperature and the chemical potential of the metal. This corresponds to the (μ,N_{H},V,T) ensemble. We compute the chemical potential at the pressure of interest, $p=0$ in this work, by thermodynamic integration.[12] In a second step, the simulation can be done in $[\mu(p),N_{\mathrm{H}},V,T]$. Since we do not know the equation of state relating pressure and volume, one has to perform a set of calculations to find the volume which would give, on average, a pressure approximately equal to the target pressure. This is inconvenient in practice. Since the number of vacancies is large when dealing with superabundant vacancies, the equilibration of the system is long. To limit the number of simulations, we leave (μ,N_{H},V,T) momentaneously and run simulations in an unphysical ensemble $[M,\mu(p),N_{\mathrm{H}},p,T]$, where the microscopic system is constrained by fixing the crystal structure and number of lattice sites M. M is an extra extensive variable which is used to stabilize the system while "relaxing" the volume. The concentration of vacancies, the distribution of vacancy-hydrogen clusters, the order parameters and the average volume $\bar{V}$ are computed. Next, the simulation is performed in $[\mu(p),N_{\mathrm{H}},\bar{V}(p),T]$ and the average virial pressure is computed (Fig. 1).

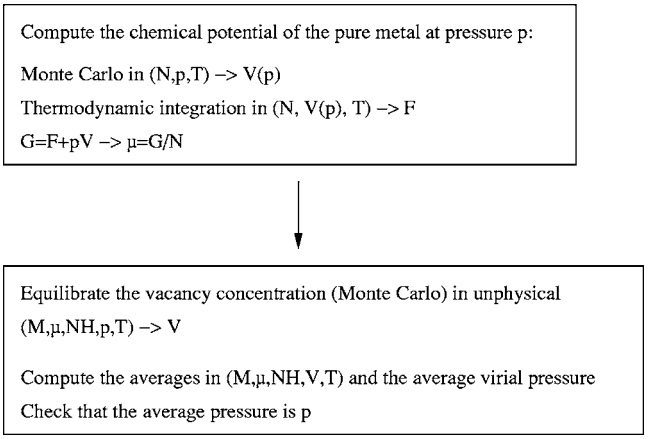

FIG. 1. A schematic representation of the different steps of the procedure to compute phase diagram points in $[\mu(p),N_{\mathrm{H}},V(p),T]$. $\mu(p)$ is the chemical potential of the pure metal at the pressure of interest. $V(p)$ is the volume of the system containing superabundant vacancies which gives on average the pressure p.

The constrained microscopic system is described by a lattice model of the Ising type where a state is characterized by the occupation numbers $\{p_n\}$ of the lattice sites. When a system is characterized by a discrete set of states with the energy $\mathcal{H}(\{p_n\})$, the partition function in (μ,V,T) is

$$\mathcal{Z}=\sum_{N=0}^{M}\sum_{\{p_n\}}\exp\{\beta[\mathcal{H}(\{p_n\})-N\mu]\}, \tag{3}$$

where p_n is 1 if site n is occupied by a particle and 0 if it is occupied by a vacancy. In order to take into account the disorder coming from the vibrations of the particles on their lattice sites, the lattice distortions due to the vacancies and eventually due to preexisting crystalline defects, we add continuous degrees of freedom to the site occupancies.[16,17] The same phase space as in the case of continuous positions in the off-lattice case is accessible to the system, except that self interstitials are not allowed. In order to change the number of particles in the same spirit as the biased insertion/removal moves of Swope and Andersen,[14] a grid is set on the physical space in order to divide it into cells which continously cover the volume V. Instead of characterizing the position of a particle n by the vector $\vec{r}_n$ from the origin, the position is given by tuning the occupation number of site n to 1 and setting the displacement from the lattice node n to $\vec{u}_n$:

$$\vec{r}_n=\vec{r}_n^{\,0}+\vec{u}_n. \tag{4}$$

The displacement $\vec{u}_n$ is confined to the cell attached to the site n. The natural choice is to use the Voronoi decomposition (Wigner-Seitz cell in the perfect crystal) to define the volume attached to each site. With this grid, vacancies are immediately localized in any microscopic configuration of the system. The transfer from the discrete partition function to the continuous case is done in the usual way[18] considering that a state defined by $\{\vec{u}_n,\vec{p}_n\}$ with accuracy $d\vec{u}^N d\vec{p}^N$, occu-

pies a volume $d\vec{u}^N d\vec{p}^N/h^3$ in a continuous phase space. The partition function is

$$\mathcal{Q}_c(M,\mu,V,T) = \sum_{N=0}^{M} \sum_{\{p_n\}} \frac{1}{\Lambda^{3N}} \int_{\mathrm{WS}} d\vec{u}^N \times \exp\{-\beta[\mathcal{H}(\{p_n\},(\vec{u})^N) - N\mu]\}, \quad (5)$$

where WS is the volume of the Wigner-Seitz cell surrounding each lattice site and Λ is the thermal de Broglie wave length $[\Lambda = \sqrt{h^2/(2\pi m k_B T)}]$, m is the mass of the particle. Note that, as in the Ising model, there is no division by $N!$, contrary to the off-lattice case.

Then we use the extra extensive variable M to free the volume, at constant crystal structure, to obtain the final partition function in a (M,μ,p,T) constrained ensemble

$$\mathcal{Q}_c(M,\mu,p,T) = \sum_{N=0}^{M} \sum_{\{p_n\}} \frac{1}{\Lambda^{3N}} \int d\lambda \lambda^{3N} \int_{\mathrm{WS}_0} d\vec{u}^N \times \exp\{-\beta[\mathcal{H}(\{p_n\},(\vec{u})^N) - N\mu - p\lambda V_0]\}, \quad (6)$$

where λ is an homotethic factor that allows volume changes at fixed crystal structure.

Phase space is sampled according to the probability densities associated with Eqs. (5) and (6) in, respectively, (M,μ,V,T) and (M,μ,p,T) ensembles. Volume changes and particle displacements are performed by selecting volume increments or displacement increments at random according to a uniform distribution, adjusting the maximum amplitude to have an acceptance rate of 50%. If the new displacement brings the particle out of the Wigner-Seitz cell, the move is rejected. The change in the number of particles is detailed in order to visualize the meaning of vacancy creation/deletion. The dilatation λ is constant. We follow Ref. 14, but in a simplified version of the algorithm, since all WS cells are ID cells in our model and we do not bias the choice of the cells. However, the lattice site occupation numbers ensure that no particle insertion is attempted in a cell that already contains a particle. A state A is characterized by $[\{p_n\},(\vec{u})^N]$. A lattice site k is chosen at random, with probability $1/M$. If the site is occupied, the occupation is set to 0 and the new trial state B is $[\{p_n, p_k=0\},(\vec{u})^{N-1}]$. In order to perform the reverse move, starting from B, one has to select the same site k. This is done with probability $1/M$. Then the particle has to be inserted at the exact position $\vec{u}_k$ where it was in state A. This is done by choosing a position in the Wigner-Seitz cell randomly. The probability of finding $\vec{u}_k$ within an error of $d\vec{u}_k$ is the ratio of the volumes $d\vec{u}_k/\mathrm{WS}_0$. Detailed balance imposes

$$\rho_A P_{A\to B} \mathrm{acc}_{A\to B} = \rho_B P_{B\to A} \mathrm{acc}_{B\to A}, \quad (7)$$

$$\frac{\lambda^{3N}}{\Lambda^{3N}} d\vec{u}^N \exp\{-\beta[\mathcal{H}(\{p_n\},(\vec{u})^N) - N\mu]\} \frac{1}{M} \mathrm{acc}_{A\to B} = \frac{\lambda^{3(N-1)}}{\Lambda^{3(N-1)}} d\vec{u}^{N-1} \exp\{-\beta[\mathcal{H}(\{p_n\},(\vec{u})^{N-1}) - (N-1)\mu]\} \frac{1}{M} \frac{d\vec{u}_k}{\mathrm{WS}_0} \mathrm{acc}_{B\to A}, \quad (8)$$

$$\frac{\mathrm{acc}_{A\to B}}{\mathrm{acc}_{B\to A}} = \exp[-\beta(\mathcal{H}_B - \mathcal{H}_A + \mu)] \frac{\Lambda^3}{\mathrm{WS}}, \quad (9)$$

where WS/Λ^3 represents the volume of phase space that is no longer accessible to the system because of the creation of a vacancy.

C. Computation of the formation free energy of a vacancy in pure Al

The equilibrium concentration of vacancies is computed by two independent ways. First, Monte Carlo simulations in (M,μ,p,T) are performed and the average vacancy concentration is computed directly at a temperature that is high enough to measure the average with enough precision. The chemical potential is set to the free energy per particle of the defect free crystal at the mean volume corresponding to zero pressure. The free energy of the crystal without defect is computed in (N,V,T) by the thermodynamic integration of Frenkel and Ladd[19] by coupling each particle to an independent harmonic oscillator attached to the lattice node. The volume is set to the average volume of the perfect crystal at $p=0$. The second calculation is done by using the Widom insertion method. Following Ref. 20, the free energy to create a vacancy (g_f^v) in (N,p,T) at the lattice node labeled k is

$$\begin{aligned} g_f^v &= G_{M+1,0}(N,p,T) - G_{M,1}(N,p,T) \\ &= G_{M+1,0}(N,p,T) - G_{M+1,1}(N+1,p,T) \\ &\quad + G_{M+1,1}(N+1,p,T) - G_{M,1}(N,p,T), \end{aligned} \quad (10)$$

where M is the number of site, and the second subscript is the occupancy of the specific site k in the lattice where the new vacancy is created. Equation (10) can be split in two parts:

$$\mu = G_{M+1,1}(N+1,p,T) - G_{M,1}(N,p,T), \quad (11)$$

where $G_{M+1,1}$ is the free energy of a system with $M+1$ sites, $N+1$ particles, and no vacancies at site k. It is related to the free energy by

$$\begin{aligned} &G_{M+1,1}(N+1,p,T) \\ &= -k_B T \ln[\mathcal{Q}_c(M+1,N+1,p,T)] \\ &= -k_B T \ln\left\{ \frac{1}{\Lambda^{3(N+1)}} \int d\lambda \lambda^{3(N+1)} \int_{\mathrm{WS}_0} d\vec{u}^{N+1} \times \exp[-\beta(\mathcal{H}(N+1) - p\lambda V_0)] \right\}. \end{aligned} \quad (12)$$

The second part of Eq. (10) gives

$$g_1 = G_{M+1,1}(N+1,p,T) - G_{M+1,0}(N,p,T)$$
$$= -k_B T \ln\left\{ \int d\lambda \lambda^{3N} \int_{WS_0} (d\vec{u})^N \frac{\exp\{-\beta[\mathcal{H}(N) - p\lambda V_0]\}}{\int d\lambda \lambda^{3N} \int_{WS_0} (d\vec{u})^N \exp\{-\beta[\mathcal{H}(N) - p\lambda V_0]\}} \int_{WS_0} d\vec{u}_k \frac{\lambda^3}{\Lambda^3} \exp[-\beta \Delta\mathcal{H}(N+1,N)] \right\}, \quad (13)$$

$$g_1 = -k_B T \ln\left\langle \int_{WS_0} d\vec{u}_k \frac{\lambda^3}{\Lambda^3} \exp[-\beta \Delta\mathcal{H}(N+1,N)] \right\rangle, \quad (14)$$

where $\Delta\mathcal{H}(N+1,N) = \mathcal{H}(N+1) - \mathcal{H}(N)$ is the potential energy difference of the system when a particle is inserted at position $\vec{u}_k$ on the site k. The square brackets denote ensemble average in the system with N particles, $M+1$ sites, and one fixed vacancy on the site k. The ensemble average is computed by Monte Carlo, and, in the meantime, the three-dimensional integral over the position of the particle k is computed on a grid.[12]

The free energy to create a vacancy is computed from Eqs. (11) and (14). The link with the equilibrium vacancy concentration (c_v) is obtained analytically for a lattice gas[20]

$$c_v = \exp(-\beta g_f^v). \quad (15)$$

Table I shows the value obtained by the two methods at high temperature, for the aluminum potential considered.[21] The agreement is excellent.

The computation of the vacancy concentration by two independent ways ensures the coherence of the method. It is a necessary intermediate step before treating superabundant vacancies in the bulk. The method has to be tested further in the case of complex defects such as grain boundaries. It has to be stressed that the decomposition of space in Voronoï cells limits the sampling of phase space. For example, configurations where two particles are so close that they fall in the same cell are forbidden. It is an approximation valid in bulk solids. Which lattice and cell decomposition has to be considered for adequately sampling the microstates of a grain boundary is an issue and the subject of further work.

TABLE I. Chemical potential at zero pressure $\mu(T,p=0)$, free energy for the formation of a vacancy obtained from Widom insertion $g_f^v(T,p=0)_W$ and from Monte Carlo simulations $g_f^v(T,p=0)_{MC}$ with Eq. (15). The Al EAM potential is taken from Ref. 21.

T	$\mu(T,p=0)$ (eV)	$g_f^v(T,p=0)_W$ (eV)	$g_f^v(T,p=0)_{MC}$ (eV)
0	−3.36	0.69	
300	−3.371	0.667	
400	−3.404	0.658	
500	−3.443	0.649	
600	−3.488	0.642	
700	−3.538	0.629	0.628
800	−3.591	0.616	0.617
900	−3.648	0.598	0.601

III. STABILITY OF SUPERABUNDANT VACANCIES: MONTE CARLO SIMULATIONS

A. Methodology

1. A generic potential for vacancy-hydrogen interaction

In the metallic systems we are interested in (the major elements of the structural alloys), the binding between the vacancy and the interstitial solute is high (Table II) with respect to the formation energy of the point defect. Furthermore, ion channeling experiments have shown that hydrogen does not occupy the center of the vacancy.[22] This raises the problem of the multiple occupancy of the vacancy and the nature of the H-H interaction inside a metal vacancy. Early electronic structure calculations[23] in free electron gas show that this interaction is repulsive unless the electronic density is low, in the vicinity of a surface, for example. In bulk metals the interaction should be repulsive. In vacancies, the semi-quantitative effective medium theory[24] predicts a repulsive interaction, that is, if an H_2 is put at the center of the vacancy, it dissociates and each H atom "occupies" an off-center position. Furthermore, the hydrogen-vacancy binding energy between H and a vacancy decreases with the occupation of the interstitial sites in the vacancy. This has been confirmed by recent *ab initio* calculations in α iron.[25] Experimental results are consistent with this picture: the redistribution and desorption of implanted hydrogen and deuterium are well interpreted in terms of multiple occupancy considering two binding energies: the energy of the isolated hydrogen in the vacancy, and a noticeably smaller one when the multiple occupation implies H-H interactions. For example, in Ni, the values are −0.44 and −0.28 eV.[26] It has an important consequence: a negative formation energy (when the reference state for H is the bulk interstitial position) of the interstitial-vacancy complex is possible in the case of

TABLE II. Formation energy $[E_f^v(\text{eV})]$ of a vacancy compared to the segregation energy $[\Delta E_{seg}(\text{eV})]$ of H to a vacancy (see Refs. 3 and 22, and references therein).

	Al	Ni	Fe	Cu
E_f^v(eV)	0.69	1.59	1.6	1.3
ΔE_{seg}(eV)	−0.51	−0.44	−0.63	−0.42

multiple occupancy. We will make reference to it by VH_n, where n is the number of interstitials within the vacancy. The number of VH_n is therefore expected to be of the order of $1/n$ of the number of H atoms in the system, that is, many orders of magnitude higher than the equilibrium concentration of vacancies in the pure metal.

The picture is not so clear concerning vacancies in Al. The work from Myers *et al.*,[26] combining H transport equations in a field of irradiation induced vacancies and results for EMT, came to a remarkable agreement concerning the binding energy to the vacancy [0.52 eV (Refs. 26 and 27)]. This value is confirmed by positron experiments.[28] However, contrary to the ion implantation experiments in Ni, multiple occupancy has not been confirmed by their experiments in Al,[27] whereas the off-center, tetrahedral, position has been observed experimentally[29] and confirmed by recent ab initio calculations.[30,31] A plausible interpretation has been proposed:[27] the ion implantation creates much greater vacancy concentrations in Al and the H is singly trapped already after implantation, even at low temperature.[29] The concentration of H cannot be increased in ion implantation experiments because high irradiation damage creates hydrogen bubbles by vacancy condensation, as observed in Ref. 27. *Ab initio* calculations[31] predict that up to 12 hydrogen atoms can be trapped in a single vacancy in Al. The H-H interaction is repulsive but the energy balance is still favorable when the reference state for H is the bulk tetrahedral interstitial site. These calculations show that the effective pair interactions between clusters come from complex electronic effects. The divacancy in pure Al is weakly unstable due to the charge redistribution between the nearest neighbors (NN) of the vacancy. VH_1-VH_1 NN interaction is repulsive (0.21 eV), whereas VH_2-VH_2 NN interaction is attractive (−0.29 eV). The explanation proposed is that the H_2 unit in the vacancy attracts more conduction electrons from the NN shell than the isolated H. This disrupts the charge redistribution at the origin of the repulsion in pure Al and leads to the condensation of the VH_2 clusters.

Reproducing these effects with a classical interatomic potential, like EAM, is difficult. Therefore, we use a generic EAM model which reproduces qualitatively some characteristics of the Al-H system. The experimental hydrogen-vacancy binding energy is reproduced. The H-H interaction is repulsive, which gives a decreasing binding energy energy with the number of H in the vacancy. The possibility of forming "H_2-like" molecules at the center of the vacancy is not possible with this potential. However, as shown below, the Monte Carlo method proposed could take these configurations into account if they were favored by the potential, since 14 interstitial sites are associated with each vacancy. We keep Al-H as a test system, because of the low value of the formation energy of the vacancies and the high binding of H, which makes this system the ideal candidate to simulate the formation of superabundant vacancies and their ordering in the bulk.

The Al EAM potential is taken from Ref. 21, as in the previous section. The Al-H model has been developed to study intergranular hydrogen segregation.[32] The potential energy profile, without relaxation, along a (111) direction across the vacancy is presented in Fig. 2. The relaxed configuration gives a segregation energy of −0.53 eV at a position shifted by $0.08a_{\mathrm{Al}}$ (0.32 Å) from the lattice tetrahedral position towards the center of the vacancy, the reference being the bulk interstitials site. These values are in qualitative agreement with the *ab initio* results, which give a segregation energy of −0.33 eV at a position shifted by 0.15 Å (Ref. 30) and −0.4 eV,[31] but the experimental binding energy is reproduced. The formation energies of the vacancy hydrogen clusters VH_n are computed at $T=0$ and $p=0$, as a function of n, where n is the number of hydrogen atoms in the vacancy, for all possible configurations of the n hydrogen atoms on the eight tetrahedral sites contained in the vacancy. Only the energy of the configurations with a low energy per H are shown in Table III. The mean segregation energy of an H to the cluster $\Delta E^{n_{\mathrm{H}}}_{\mathrm{seg}}$ decreases (in absolute value) with n_{H} as expected from the repulsive H-H interaction. Please note that this variation is larger and nonmonotonous in *ab initio* Al-H.[31] The formation energy of the cluster per hydrogen atom ($E^c_f = E^l_f/n_{\mathrm{H}} + \Delta E^{n_{\mathrm{H}}}_{\mathrm{seg}}$, where E^l_f is the formation energy of

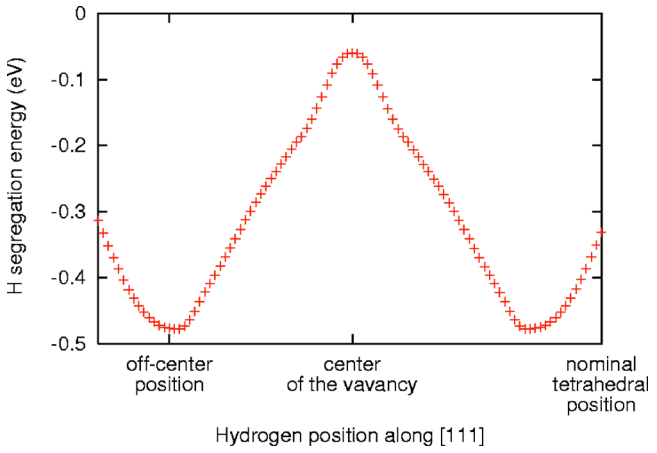

FIG. 2. (Color online) Hydrogen segregation energy profile in eV along [111] in a vacancy. The minimum potential energy is obtained for an off-center position.

TABLE III. Vacancy-hydrogen clusters' configurations obtained with the EAM model (Ref. 32). The mean segregation energy of one hydrogen to the configuration $\bar{\Delta}E^{n_{\mathrm{H}}}_{\mathrm{seg}}$(eV/at), the formation energy per hydrogen atom $[E^c_f = E^l_f/n_{\mathrm{H}} + \bar{\Delta}E^{n_{\mathrm{H}}}_{\mathrm{seg}}$(eV/at)], and the degeneracy of the microstate ($n^{n_{\mathrm{H}}}$) are given. n_{H} is the number of H in the cluster.

n_{H}	$\bar{\Delta}E^{n_{\mathrm{H}}}_{\mathrm{seg}}$(eV)	E^c_f(eV/at)	$n^{n_{\mathrm{H}}}$
0	0	0.69	1
1	−0.53	0.159	8
2	−0.52	−0.18	4
3	−0.49	−0.26	8
4	−0.43	−0.26	28
5	−0.40	−0.27	8
6	−0.36	−0.25	4
7	−0.32	−0.22	8
8	−0.29	−0.2	8

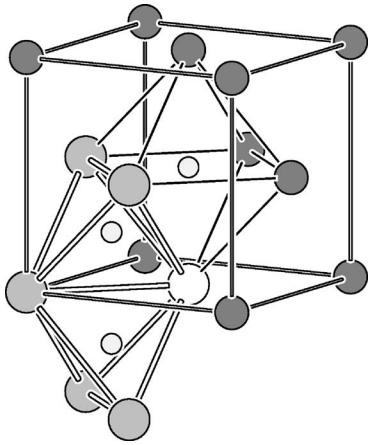

FIG. 3. fcc structure with two of the eight tetrahedral positions and one of the six octahedral positions associated with a vacancy (big white circle).

the vacancy without H) is the quantity which gives the stability of the clusters when (n_H, μ, V, T) are imposed. Table III shows that $V\mathrm{H}_3$, $V\mathrm{H}_4$, and $V\mathrm{H}_5$ are within 10 meV in energy. Therefore, the three clusters should exist together at high temperature. From this rough analysis at $T=0$ it is clear that a Monte Carlo simulation of the $V\mathrm{H}_n$ stability has to deal with a mixture of different clusters and has to be designed to sample as efficiently as possible all the different configurations of a single vacancy, i.e., not only a fluctuating number of hydrogen (n_H fluctuation), but also all the permutation of occupancies between the interstitial sites of the vacancy. The second important aspect of the simulation is the interaction between the clusters. Pair interactions (ϵ_1), with relaxations, are evaluated by taking the difference of potential energy between two configurations. In the first one, the two clusters are far enough to have a negligible interaction, whereas in the second one, they are placed in first neighbor positions. For this Al potential the divacancy is weakly favored compared to single vacancies ($\epsilon_1=-10$ meV), whereas the $V\mathrm{H}_8$ clusters have strongly repulsive interactions ($\epsilon_1=0.91$ eV). This can be easily understood from the geometry of the clusters. Two first neighbors on the fcc lattice have in common two tetrahedral interstitial first neighbors (Fig. 3). When two vacancies are first neighbors, each of these interstitial sites can be occupied by two H atoms, each one displaced towards the center of one vacancy. Therefore, one nominal tetrahedral site is split in two off-center sites. This is the situation that occurs when two $V\mathrm{H}_8$ clusters are put in first neighbors position, so there is a strong repulsion coming from the H-H interaction. On the contrary, when two $V\mathrm{H}_3$ clusters are brought in first neighbors positions, it is possible to arrange the hydrogen atoms in such a way that the double occupancy is avoided. In this case, the attraction is large ($\epsilon_1=-0.1$ eV). As a consequence, a $V\mathrm{H}_n$ demixion can be expected at low temperature if the stable cluster at that temperature has a low number of hydrogen n. It can be noticed that the strong repulsion between $V\mathrm{H}_6$ clusters has been observed experimentally[33] in Ni-H, where the SAV get ordered in the $L1_2$ structure at 25 at. % SAV, therefore avoiding being in first neighbor position. Again, the analysis at $T=0$ stresses important effects which have to be included in the simulation: the double occupancy of the interstitial positions should be allowed, the ordering of the clusters and the hydrogen configuration within a vacancy (number and arrangement) are bound. We chose to resolve the double occupancy problem by designing a new interstitial network where the nominal interstitials sites are split between their first neighbors in the fcc lattice. With this new network, each vacancy contains 8 tetrahedral and 6 octahedral sites. Such description gives more room to the off-center H positions. In the next section, the new network for interstitials is explained and the H part of the Monte Carlo method is detailed.

2. Monte Carlo moves

The objective of the simulations is to make a rough estimate of the phase diagram of SAV, in the range of concentrations relevant to hydrogen damage in aqueous environments ($C_H \in [500\ \mathrm{ppm}, 1\%]$ in Al) and for temperatures down to 300 K. For this reason, we impose the number of hydrogen particles in the system and not the chemical potential of H_2. As discussed previously, imposing p and μ_{Al} at the same time does not correspond to a thermodynamic state, so we approximate the $(N_{Al}, N_H, p=0, T)$ macroscopic conditions by equilibrating the system by Monte Carlo simulations in $[M, \mu_{Al}(p=0), N_H, p=0, T]$ according to the partition function (6) and compute the concentration of vacancies, the distribution of $V\mathrm{H}_n$ and the average volume $\bar{V}$. Next, we perform Monte Carlo simulations in $[M, \mu_{Al}(p=0), N_H, \bar{V}, T]$ and check that the average virial pressure is close to zero within a few MPa.

The discussion above raises two technical problems: the configuration of the individual $V\mathrm{H}_n$ (number of hydrogen atoms inside the vacancy and their arrangement) have to be sampled at the same time as the location of the vacancy in the metal lattice, in order to describe the ordering correctly. Many Monte Carlo moves have to be considered.

(i) The volume changes and the preliminary $[M, \mu(p), N_H, p, T]$ simulation are necessary because the equation of state is not known.

(ii) The position of the metal and hydrogen particles are sampled to take into account local distortions (stress fields).

(iii) The insertion and removal of particles are used to equilibrate the vacancy concentration (see Sec. II B).

(iv) The exchange of a vacancy with a metal particle on the metal lattice enables the vacancies to order.

(v) The exchange of a hydrogen atom with a vacancy on the interstitial network samples the $V\mathrm{H}_n$ configurations.

Let us first consider the cluster ordering because it gives the motivation for introducing a new network structure with a subdivision of the volume in Wigner-Seitz cells. This structure influences all the Monte Carlo moves. Let us imagine that the number of vacancies is fixed and that they are decorated with hydrogen. It is obvious that exchanging a vacancy without moving the entire entity "vacancy plus included hydrogens" will always be rejected. If one tries to exchange the vacancy alone, all the hydrogens will be set to bulk interstitial positions and the energy cost of the move will be of the order of $-n\Delta E_{seg}$, where the segregation energy ΔE_{seg} is of

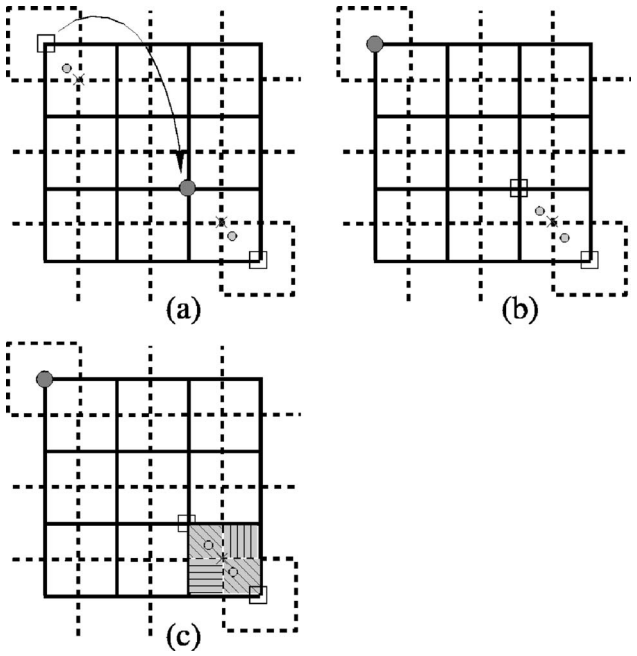

FIG. 4. A two-dimensional square lattice (full lines), and the interstitial lattice (dashed lines), the empty squares represent vacancies, the big gray circle a particle and the small gray circles are hydrogen atoms. (a) Exchange of VH_1 with a particle. (b) The two hydrogen atoms share the same lattice site (cross). (c) The interstitial lattice site is split in four between its neighbors. The dashed areas represent the Wigner-Seitz cell of the new interstitial sites.

the order of −0.4 eV (Table III). The idea is to perform a "cluster move"[12,34] by exchanging the vacancy-hydrogen cluster, as a single entity, with another specie occupying another metal lattice site. Let us define what we mean by "inside" the vacancy. It means that each hydrogen atom which is inside the Wigner-Seitz cell surrounding the lattice site hosting the vacancy is considered as being part of the cluster to be exchanged. The exchange cluster move has to satisfy the detailed balance

$$\rho_1 P_{1\to 2} \mathrm{acc}_{1\to 2} = \rho_2 P_{2\to 1} \mathrm{acc}_{2\to 1}, \tag{16}$$

where ρ_1 is the equilibrium probability of being in state 1, $P_{1\to 2}$ is the *a priori* probability of proposing a transition from state 1 to state 2, and $\mathrm{acc}_{1\to 2}$ is the probability of accepting the transition. A vacancy and a metal lattice site are selected at random with probability $(1/N_{\mathrm{vac}})(1/M)$ (N_{vac} is the number of vacancies in the system in state 1, and M is the fixed number of metal lattice site). The number of hydrogen particles lying in the Wigner-Seitz cell of each site are found and exchanged together with the occupancies on the lattice sites (the displacements from the nodes are not changed). The advantage of considering the Wigner-Seitz cell is that there is no overlap between the clusters, therefore the distribution of the hydrogens over the vacancies is still the same in state 2 as in state 1. The reverse move can be proposed with the same probability. The problem is that the interstitial sites lie on the border of the Wigner-Seitz cell.

Consider the case of a two-dimensional square lattice. The interstitial lattice is also square (dashed lines in Fig. 4). Figure 4 shows the example of an exchange between a cluster and a particle [Fig. 4(a)]. The exchange brings two clusters in second neighbor position where they share the same interstitial site [Fig. 4(b)]. This move brings two hydrogen atoms on the same lattice site, each of them being shifted towards its vacancy according to the potential energy landscape within the isolated vacancy (Sec. III A 1). Occupancies greater than 1 would introduce redundancies in the way the microstates are counted since the interstitial particles are indistinguishable [a microstate where H_1 has a displacement u_1 and H_2 has a displacement u_2 is the same as the state (H_1,u_2), (H_2,u_1) if both particles share the same lattice site]. In the model proposed, the interstitial sites are split between their first neighbors. The volume accessible for the displacement of the H particles is simply the intersection of the interstitial Wigner-Seitz cell with the Wigner-Seitz cell of the metal lattice [Fig. 4(c)]. In the fcc structure, each lattice site "contains" eight such tetrahedral sites and six octahedral sites. Another problem arises from this definition: the hydrogen particles can jump from one site to the other by random displacements. The displacement moves are done as follows: an increment of displacement is chosen at random and added to the current value of the displacement. If the particle crosses the limit of its cell towards a target site, the occupancy of this site is considered. If the site is empty, the jump is accepted according to the Metropolis criterion. The new state is the one with the target site occupancy switched to 1 and the occupancy of the original site switched to 0. The displacement of the particle is simply referenced from the new site. If the target site is already occupied, the new state will contain a double occupancy. This is not allowed in the model, so the probability of such a state is zero. Therefore, detailed balance gives a zero acceptance probability for such a move [set ρ_2 to zero in Eq. (16)]. The move is rejected.

The cluster moves are essential to study the ordering tendencies. They are highly dependent on the configuration of the cluster. Therefore, it is necessary to sample the configuration of a single cluster as efficiently as possible at the same time as the cluster moves are performed. This is done in two ways: by proposing displacement moves to the hydrogen particles, as shown above, or by performing exchanges between occupied and empty interstitial sites. The exchange of H atoms is performed by choosing one H particle at random, then choosing the new interstitial location at random and one of its 14 interstitials sites randomly. If the site is already occupied, the move is rejected. If not, the exchange is accepted according to the metropolis rule. The "target" interstitial position is always chosen by the intermediate of a "target" metal lattice site because the $14\times M$ interstitial sites are not allocated: the interstitial network is only constructed in the vicinity of the metal site which hosts the interstitial. Therefore, only $14\times N_{\mathrm{H}}$ sites at maximum are physically allocated in the computer memory. This means that working with interstitials on a lattice does not require significantly more memory than working with a pure metal, as long as the concentration is low. Furthermore, a large proportion of the exchanges are performed between interstitial sites belonging to vacancies, when the concentration of hydrogen remaining in the bulk is small (the segregation energy to the vacancy is large, of the order of −0.5 eV). An additional trick is used to

increase the acceptance rate of these exchanges: biased insertions. It is detailed in the Appendix.

The main loop in the Monte Carlo simulation is dedicated to proposing different types of moves according to the probabilities: pdr_{Al} (displacement of an Al particle), pdr_{H} (displacement of an H particle), pAB (change of occupancy on the metal lattice, i.e., creation/removal of vacancies), pX (exchange of a H particle), and pC (cluster move). The values of these parameters are set empirically in order to equilibrate the system, the influence on the averages and the acceptance rates are controlled. A typical set of parameters is $pdr_{\mathrm{Al}}=0.1$, $pdr_{\mathrm{H}}=0.01$, $pAB=0.45$, $pX=0.07$, and $pC=0.37$. In practice we found that the effect of the choice of the proportion of the various steps is not critical in comparison to the severe decrease of the acceptance ratio of cluster and exchange moves when short-range order appears. This phenomenon, known as the "critical slowing down," is rooted in the physics of phase transitions.

B. Superabundant vacancies and local ordering: the Al-H system

1. Computational details

The simulations were performed in perfect crystals containing $16\times16\times16$ unit cells (16 364 fcc lattice sites) with 160 hydrogen atoms ($C_{\mathrm{H}}=1\%$), $32\times32\times32$ unit cells (131 072 fcc lattice sites) and 130 hydrogen atoms ($C_{\mathrm{H}}=1000$ ppm) and, finally, $64\times32\times32$ unit cells (262 144 fcc lattice sites) and 130 hydrogen atoms ($C_{\mathrm{H}}=500$ ppm). The box has periodic boundary conditions in every direction. At each macrostep, the total number of vacancies, the number of $V\mathrm{H}_n$ ($n\in[0,14]$), the virial pressure, the order parameters, and the size distribution of the vacancy clusters are measured. A macrostep is composed of 10^4 microsteps when the system is small ($C_{\mathrm{H}}=1\%$) and up to 10^6 microsteps when the order is important (at $T=300$ K and $C_{\mathrm{H}}=1\%$) or when the system is large. The measurement of the averages begins when the concentrations of $V\mathrm{H}_n$ have converged and lasts until the vacancy cluster distribution has converged. This can be quite fast when the short range order between vacancies is not important, typically 10^9 microsteps at $T=500$ K and higher temperatures or somewhat painful when there is ordering, up to 10^{11} microsteps at $T=300$ K and $C_{\mathrm{H}}=1\%$.

The short-range order parameter (Warren Cowley parameter[35]) is

$$\alpha_{nm}=\frac{\langle p_n p_m\rangle}{\langle p_n\rangle\langle p_m\rangle}-1=\frac{\langle p_n p_m\rangle}{c^2}-1, \tag{17}$$

where p_n is the occupation number on site n, which is one when the site is occupied by a vacancy, zero otherwise, and c is the concentration of vacancies. α is positive if, on average, the pair nm involves two vacancies more often than in a random solution at concentration c. Therefore, if α is positive over some range of interactions, the system has a tendency to form clusters of vacancies (demixion).

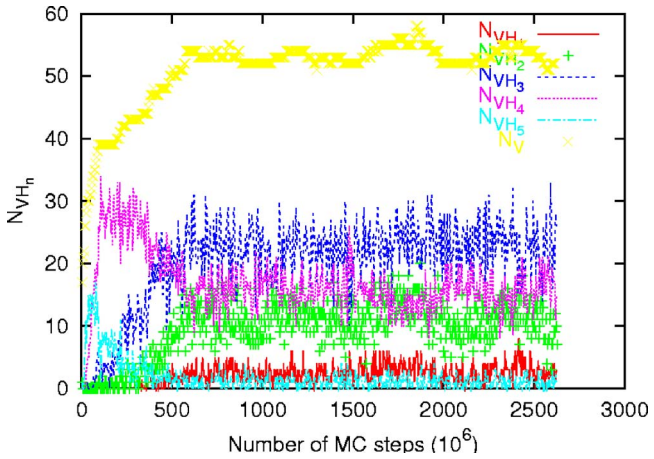

FIG. 5. (Color online) Convergence of the number of hydrogen-vacancy clusters $V\mathrm{H}_n$ for $n\in[1,5]$ and total number of vacancies as a function of the number of Monte Carlo steps at $T=400$ K and $C_{\mathrm{H}}=1\%$.

2. Superabundant vacancies at $C_{\mathrm{H}}=1\%$

In Fig. 5, the convergence of the total number of vacancies and of the number of $V\mathrm{H}_n$ are shown, as a function of the number of Monte Carlo steps at $T=400$ K and $C_{\mathrm{H}}=1\%$. The average hydrogen concentration is $C_V\sim3300$ ppm, which corresponds to one third of the hydrogen concentration. More precisely, the $V\mathrm{H}_n$ distribution [Fig. 6(c)] shows that the dominant clusters are $V\mathrm{H}_2$, $V\mathrm{H}_3$, and $V\mathrm{H}_4$. A typical microstate is represented in Fig. 6(a). There is a noticeable ordering of the vacancies in the form of chains along the $\langle110\rangle$ direction. This is confirmed at $T=300$ K, where the chains are longer [Fig. 6(b)]. However, the ordering is only short range. The comparison of the $V\mathrm{H}_n$ distribution at these temperatures shows that $V\mathrm{H}_2$ is most probable at low temperature [Figs. 6(c) and 6(d)]. The degree of short-range order is characterized here by the distribution of the mean length of the chains. At each macrostep, the number of chains is counted as a function of the chain length. This number is multiplied by the number of atoms in the chain in order to give a clearer image of the convergence at the long chain lengths. This gives the average fraction of vacancies contained in a chain of length n_{vac} [Figs. 6(e) and 6(f)]: $\langle N_{\mathrm{chains}}(n_{\mathrm{vac}})\rangle\times n_{\mathrm{vac}}/\langle N_{\mathrm{vac}}\rangle$. At $T=400$ K, the probability goes to zero shortly after $n_{\mathrm{H}}=10$. -40% of the vacancies are monovacancies whereas the chains of length 13 represent less that 6×10^{-5} of the vacancies [Fig. 6(e)], which means that one has to consider a big system of $(0.1\ \mu\mathrm{m})^3$ to have at least one of these chains in the system. The histogram at $T=300$ K shows the spreading when the system aproaches the demixion domain. Reasonable statistics can be obtained, even if the ordered domains can be as large as 40 vacancies [Fig. 6(f)], which means that the method is adequate for simulating local structure changes.

The effect of the potential on the ordering has been tested by modifying the hydrogen-hydrogen repulsive interaction. The potential was initially fitted[32] on the calculation of the potential energy of two hydrogen atoms immersed in an electron gas. The pair interaction has two parameter Z and α:

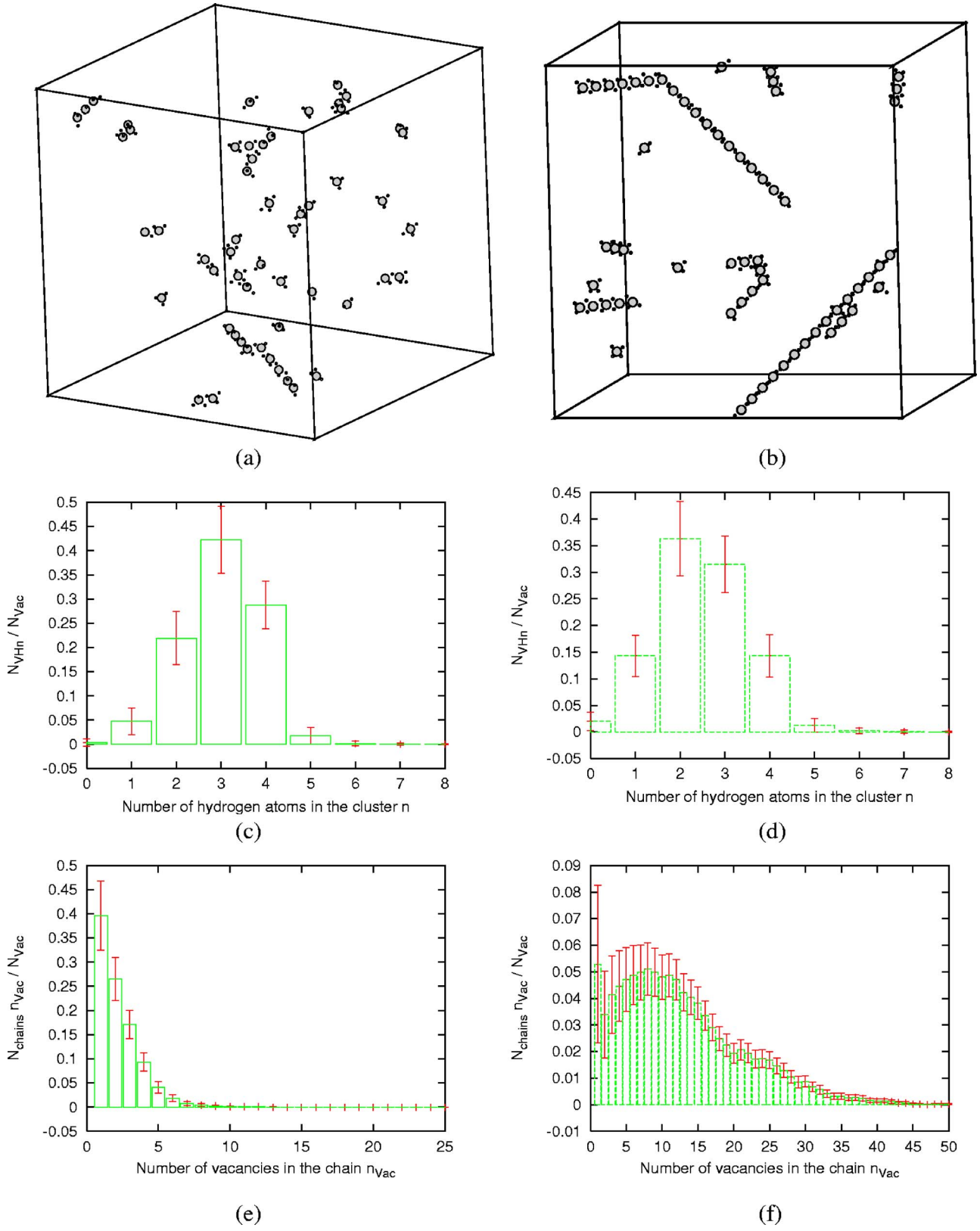

FIG. 6. (Color online) Typical microstates of the system at $C_H=1\%$ and $T=400$ K (a) and $T=300$ K (b) are shown. The large circles (small) represent vacancies (hydrogen atoms). The radius of the vacancies is shortened in order to visualize the hydrogen atoms located inside. The Al atoms are not represented. Note the increasing short range order along ⟨110⟩ directions. The equilibrium distribution of VH_n at $T=400$ and 300 K are represented in (c) and (d), respectively, as well as the histograms showing the probability that a vacancy belongs to a chain of length n, as a function of n, the number of vacancy in the cluster [at $T=400$ K (e) and $T=300$ K (f)]. The bars represent the mean square deviation (fluctuation amplitude), the error is less than 10^{-3} for the VH_n distributions.

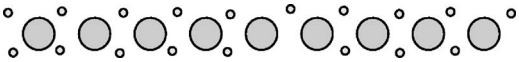

FIG. 7. A VH_2 chain lying along $\langle 110\rangle$, viewed from $\langle \bar{1}10\rangle$. All the hydrogen particles are in the plane $(\bar{1}10)$. The picture is a zoom of Fig. 6(b).

$$V_{\text{H-H}}(r) = \frac{Ze^{-\alpha r}}{r} \tag{18}$$

fitted on two values of the energy at two distances. At short distances ($r_{\text{H-H}}=0.2a_{\text{Al}}$), we keep the high repulsion energy found by in the electron gas $(0.8\ \text{eV})^2$ and at the first neighbor distance ($r_{\text{H-H}}\approx 0.5a_{\text{Al}}$ between two tetrahedral sites) the repulsion is, for the three potentials tested here, 0.09, 0.05, and 0.025 eV. The interaction is brought to zero continuously by a fifth order polynomial between $0.6a_{\text{Al}}$ and $0.8a_{\text{Al}}$. A closer look at the chain configuration (Fig. 7) shows that the vacancy-hydrogen clusters are VH_2. Each vacancy pair shares two hydrogen atoms which are in first neighbor position. Adding one hydrogen more in the vacancy at a tetrahedral position would create two more H-H first neighbor pairs and is therefore unfavorable when the repulsion is high. This has been confirmed by the use of the potentials with decreased repulsive interaction, where the chain structure is conserved, but more H can be added in a chain. The same increase in first neighbor interactions would occur if two chains are gathered in order to form platelets. When the repulsion is decreased, the critical temperature for demixion is increased and platelets along {111} and {100} are obtained, together with chains along $\langle 110\rangle$. Demixion occurs above $T=300$ K and therefore no statistics can be obtained at this temperature where the system is trapped in a configuration which depends on the starting point. Nevertheless significant data can be obtained at $T=400$ K, where the order is still short range. An example of a typical {100} platelet is shown in Fig. 8.

C. Influence of temperature and hydrogen concentration

At $C_{\text{H}}=1\%$, the order parameter (Fig. 9) and VH_n distribution (Fig. 10) are computed as a function of temperature.

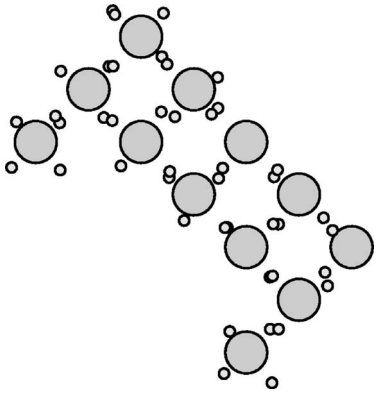

FIG. 8. VH_n clusters ordered in the shape of a platelet lying along a {100} plane. The horizontal and vertical directions are [100] directions. This configuration is obtained when the H-H repulsion is weak.

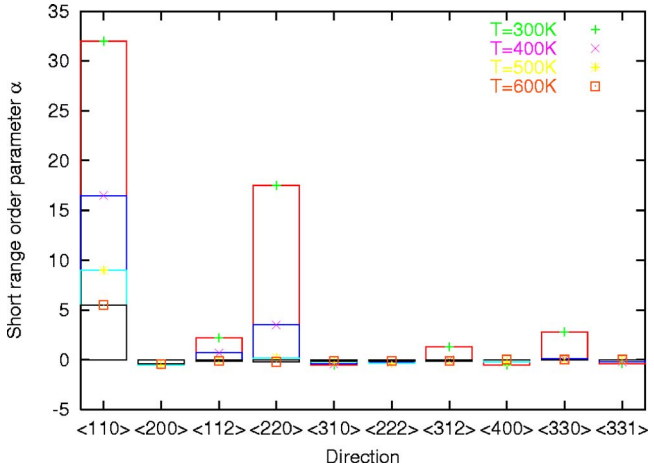

FIG. 9. (Color online) Temperature evolution of the short-range order parameter on the neighbor sites between the first and the tenth neighbor. Note the rise of the peaks at vectors $\langle 110\rangle$, $\langle 220\rangle$, and $\langle 330\rangle$ as the temperature decreases.

In agreement with the formation of VH_2 chains along $\langle 110\rangle$ directions, peaks at $\langle 110\rangle$, $\langle 220\rangle$, and $\langle 330\rangle$ positions appear when the temperature is decreased. The short-range order is still noticeable at high temperatures where the probability to find two vacancies in first neighbor position is still higher than in a random solution. Contrary to thermal vacancies, the temperature does not have a strong influence on the concentration of superabundant vacancies (Fig. 10). The influence on the distribution of VH_n is weak, VH_2 and VH_3 are the most stable in $(\mu, N_{\text{H}}, V, T)$ conditions, with a preference for VH_2 at low temperature, related to the formation of the chains. As discussed above, lowering the repulsive interaction would shift the distributions towards higher hydrogen multiple occupancies.

The influence of the hydrogen content is tested on bigger systems, up to 200 000 metal particles. Smaller concentrations like 1000 and 500 ppm are reached. These concentrations drastically decreased the degree of order in the system, and increased the hydrogen occupancy of the vacancy, which is consistent with the analysis above.

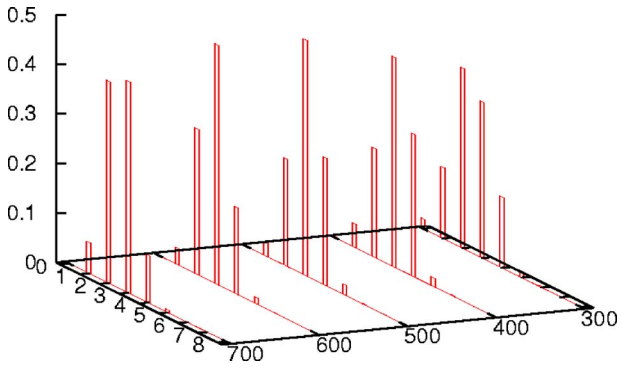

FIG. 10. (Color online) Temperature evolution of the concentration of VH_n at $C_{\text{H}}=1\%$. Note that VH_3 is the most stable vacancy-hydrogen cluster, except at low temperature where the ordering in chains favors VH_2.

TABLE IV. Influence of the temperature T and the insertion bias on the H exchange acceptance ratio R_X and influence of the temperature on the acceptance ratio R_C of the cluster moves. The hydrogen concentration is $C_H=1\%$, the other parameters of the simulation are $pX=10\%$ pC, $pdr=0.1$, $pdr_H=10C_H pdr$, $pdV=0.0005$, $nat_{Al}=16384$, $p=0$, $\mu_{Al}=\mu_{Al}(p,T)$.

T (K)	R_X unbiased	R_X biased	R_C
300	3×10^{-4}	1.6×10^{-3}	3.5×10^{-3}
400	2.7×10^{-3}	6×10^{-3}	10^{-2}
500	9×10^{-3}	1.5×10^{-2}	2.5×10^{-2}
600	2×10^{-2}	2.6×10^{-2}	4×10^{-2}
700	3.7×10^{-2}	4.1×10^{-2}	5×10^{-2}

IV. CONCLUSION

The main goal of this work is to develop a Monte Carlo method capable of handling the equilibration and ordering of vacancies, including the displacements of the particles. The method combines lattice site occupancies and continuous variables. The last ones describe the translational degrees of freedom of the particles. The lattice is used to perform insertion/removal Monte Carlo moves for vacancy equilibration, as well as cluster moves where a vacancy and the hydrogen atoms it contains are exchanged, as a single entity, with a metal particle. The stress field of the interstitials and of the vacancies are taken into account by the continuous variables. The method, which is tested here in the bulk, can be extended to include dislocations and interfaces, with a limited amount of work.

The potential is a generic EAM model which reproduces the main characteristics of the vacancy-hydrogen interaction as it is given by effective medium theory: the vacancy-hydrogen binding is large, multiple occupancy of the vacancy is possible, and the H-H interaction is repulsive. With this scheme, Monte Carlo simulations in (μ_{Al},N_H,V,T) at $C_H=1\%$ show that VH_2 and VH_3 vacancy-hydrogen clusters are stable and that they form $\langle 110\rangle$ chains at room temperature. Furthermore, when the H-H repulsion is weakened, nanoscale {111} and {100} platelets are formed. The predictive capacity of the model has to be taken cautiously, owing to its simplicity, in particular in Al.[31]

In bulk Al, charged electrochemically with hydrogen, ordering along {111} planes is suspected experimentaly.[10] It is likely that these ordered domains are far from equilibrium and that they are the result of the diffusion and condensation of mobile VH_1 clusters. This case is out of reach of our method based on equilibrium simulations. However, it has proved efficient enough to get statistics in the case of noticeable short range order. It is therefore a valuable tool to explore qualitatively the role of superabundant vacancies in the loss of cohesion of metallic materials, especially when H is located at interfaces, where the kinetic of H diffusion and vacancy production might be fast enough to be described by equilibrium simulations.

ACKNOWLEDGMENTS

The authors would like to thank their colleague Titus Van Erp (CECAM, ENS-Lyon) for support and for reviewing the manuscript.

APPENDIX: BIASED INSERTIONS

When an exchange move is performed, a hydrogen particle and a vacant interstitial site are chosen at random. The hydrogen atom is removed from its original site and inserted at a random position in the Wigner-Seitz cell of its new site. Most of these positions correspond to high potential energies and the moves are rejected. A way of increasing the acceptance ratio is to bias the insertion by not choosing the position at random. The biased insertion is used only when the particle is moved from one vacancy to another. Ideally, the new position should be chosen with a probability which is the statistical weight of the new microstate

$$W_n=\frac{\exp[-\beta U(r_H^n)]}{\mathcal{Q}}, \tag{A1}$$

where $U(r_H^n)$ is the potential energy of the system with the hydrogen atom at position r_H^n in the new vacancy. The reverse move, from position r_H^n inside the new vacancy to the old position r_H^o inside the original vacancy, has to be considered in order to satisfy detailed balance. It should be selected with the probability

$$W_o=\frac{\exp[-\beta U(r_H^o)]}{\mathcal{Q}}. \tag{A2}$$

Detailed balance gives

$$\rho_o W_n \mathrm{acc}_{o\to n}=\rho_n W_o \mathrm{acc}_{n\to o}. \tag{A3}$$

The cancellations in the detailed balance give an acceptance of 1. Of course, it is not possible to do this, but one can mimic this process following the Rosenbluth scheme. A set of k trial positions is generated at random. A new position is chosen with probability $W_n/\Sigma_{i=1}^k W_i$, where $W_n=\exp[-\beta\tilde{U}(r_H^n)]$ and $\tilde{U}$ is a computationally cheap estimate of the energy. For the reverse move, a set of $k-1$ positions are chosen at random, and position r_H^o is chosen with probability $W_o/(\Sigma_{i=1}^{k-1}W_i+W_o)$. Detailed balance gives

$$\frac{\mathrm{acc}_{o\to n}}{\mathrm{acc}_{n\to o}}=\frac{\sum_{i=1}^{k} W_i}{\sum_{i=1}^{k-1} W_i+W_o}\exp(-\beta\Delta U)\exp(\beta\Delta\tilde{U}). \tag{A4}$$

If $\Delta\tilde{U}$ is a good approximation of ΔU, the acceptance can be higher. We chose to approximate the energy by tabulating the energy to insert a hydrogen particle in a vacancy at different positions in the Wigner-Seitz cell at $T=0$, without relaxation. The increase in acceptance rate at different temperatures is rather modest (Table IV), except at low temperature, where a boost factor of 5 is found. This seems consistent if one considers that the exchange energy is approximated by the segregation energy difference at zero temperature.

*Electronic address: tanguy@emse.fr

[1] Y. Fukai and N. Ōkuma, Phys. Rev. Lett. **73**, 1640 (1994).
[2] Y. Fukai, Y. Shizuku, and Y. Kurokawa, J. Alloys Compd. **329**, 195 (2001).
[3] Y. Fukai, J. Alloys Compd. **356-357**, 263 (2003).
[4] H. Osono, T. Kino, Y. Kurokawa, and Y. Fukai, J. Alloys Compd. **231**, 41 (1995).
[5] Y. Fukai, M. Mizutani, S. Yokota, M. Kanazawa, Y. Miura, and T. Watanabe, J. Alloys Compd. **356-357**, 270 (2003).
[6] H. K. Birnbaum, C. Buckley, F. Zeides, E. Sirois, P. Rozenak, S. Spooner, and J. S. Lin, J. Alloys Compd. **253-254**, 260 (1997).
[7] C. E. Buckley, H. K. Birnbaum, D. Bellmann, and P. Staron, J. Alloys Compd. **293-295**, 231 (1999).
[8] A. David, G. Kögel, P. Sperr, and W. Triftshäuser, Phys. Rev. Lett. **87**, 067402 (2001).
[9] W. Egger, G. Kögel, P. Sperr, W. Triftshäuser, J. Bär, S. Rödling, and H.-J. Gudladt, Mater. Sci. Eng., A **387-389**, 317 (2004).
[10] P. Rozenak, E. Sirois, B. Ladna, H. K. Birnbaum, and S. Spooner, J. Alloys Compd. **387**, 201 (2005).
[11] W. C. Swope and H. C. Andersen, Phys. Rev. A **46**, 4539 (1992).
[12] D. Frenkel and B. Smit, *Understanding Molecular Simulation* (Academic Press, New York, 2002).
[13] K. Bagchi, H. C. Andersen, and W. Swope, Phys. Rev. Lett. **76**, 255 (1996).
[14] W. C. Swope and H. C. Andersen, J. Chem. Phys. **102**, 2851 (1995).
[15] M. Mezei, Mol. Phys. **40**, 901 (1980).
[16] B. Dünweg and D. P. Landau, Phys. Rev. B **48**, 14 182 (1993).
[17] M. Presber, B. Dünweg, and D P. Landau, Phys. Rev. E **58**, 2616 (1998).
[18] D. A. McQuarrie, *Statistical Mechanics* (Harper & Row, Boston, 1976).
[19] D. Frenkel and A. J. C. Ladd, J. Chem. Phys. **81**, 3188 (1984).
[20] S. Pronk and D. Frenkel, J. Phys. Chem. B **105**, 6722 (2001).
[21] F. Ercolessi and J. B. Adams, Europhys. Lett. **26**, 583 (1994).
[22] S. M. Myers, M. I. Baskes, H. K. Birnbaum, J. W. Corbett, G. G. Deleo, S. K. Estreicher, E. E. Haller, P. Jena, N. M. Johnson, R. Kirchheim, S. J. Pearton, and M. J. Stavola, Rev. Mod. Phys. **64**, 559 (1992).
[23] J. K. Nørskov, Phys. Rev. B **20**, 446 (1979).
[24] J. K. Nørskov and F. Besenbacher, J. Less-Common Met. **130**, 475 (1987).
[25] Y. Tateyama and T. Ohno, Phys. Rev. B **67**, 174105 (2003).
[26] S. M. Myers, P. Nordlander, F. Besenbacher, and J. K. Nørskov, Phys. Rev. B **33**, 854 (1986).
[27] S. M. Myers, F. Besenbacher, and J. K. Nørskov, J. Appl. Phys. **58**, 1841 (1985).
[28] S. Linderoth, H. Rajainmaki, and R. M. Nieminen, Phys. Rev. B **35**, 5524 (1987).
[29] J. P. Bugeat, A. C. Chami, and E. Ligeon, Phys. Rev. Lett. **58**, 127 (1976).
[30] C. Wolverton, V. Ozoliņš, and M. Asta, Phys. Rev. B **69**, 144109 (2004).
[31] G. Lu and E. Kaxiras, Phys. Rev. Lett. **94**, 155501 (2005).
[32] D. Tanguy and T. Magnin, Philos. Mag. **83**, 3995 (2003).
[33] Y. Fukai, *The Metal Hydrogen System* (Springer, Berlin, 1993).
[34] D. Wu, D. Chandler, and B. Smit, J. Phys. Chem. **96**, 4077 (1992).
[35] F. Ducastelle, *Order and Phase Stability in Alloys* (North-Holland, Amsterdam, 1991).